Analysis of the initial phase of current quenches in the DIII-D tokamak

Y. Shibata[1], M. Okamoto[2], N. Eidietis[3], K.Y. Watanabe[4], V. Lukash[5], R. Khayrutdinov[5]

[1] *National Institute of Technology, Gifu college, Motosu, Japan*

[2] *National Institute of Technology, Ishikawa college, Tubata-cho, Japan*

[3] *General Atomics, San Diego, United States of America*

[4] *National Institute for Fusion Science, Toki, Japan*

[5] *Kurchatov Institute, Moscow, Russia*

1. Introduction

Disruptions are one of the most critical issues for realization of DEMO reactor. During the current quench (CQ), the plasma current (I_p) decays rapidly because of the sudden increase in plasma resistance following the thermal quench (TQ). The rapid current decay generates potentially damaging eddy currents and electromagnetic force in conducting materials around plasma. To reduce these effects, Massive Gas Injection (MGI) and Shattered Pellet Injection (SPI) are candidate methods to mitigate the effects of TQ and CQ in ITER [1]. In this study, we focused on the initial phase of the CQ (between 100% to 80% of maximum I_p in CQ) to determine the mechanism governing the CQ decay time. In a previous study on JT-60U, it was found that there was also fast current decay during the initial phase of CQ in a high electron temperature T_e disruption discharges (T_e at the plasma center: over 100eV) and I_p decay varied with the change in plasma inductance L_p during the CQ, especially internal plasma inductance L_i [2]. And it was found from analysis of disruption simulation code that existence of T_e profile during CQ was important to generate an increase of L_i [3]. However, the verification of current decay model by using experimental data in other tokamak devices is necessary for understanding of current decay physics in disruption because these verifications were only carried out in JT-60U. In this study, we analyzed CQ in 3 types of DIII-D disruptions (low-q, error field and shell pellet injection) to confirm the impact of the time evolution of the L_i on the decay time of the CQ.

2. Experimental Results

In this study, we analyzed CQ in 3 types of DIII-D disruptions. Typical plasma parameters are as follows; Shell pellet injection (6 shots): I_p = 1.6 MA, B_t = 2.15 T, R_0 =1.72 m, a = 0.6 m, κ = 1.8, low-q: I_p = 1.89 - 2.11 MA, B_t = 1.98 T, R_0 =1.73 m, a = 0.59 m, κ = 1.81, error field: I_p = 1.63 MA, B_t = 1.97 T, R_0 =1.73 m, a = 0.59 m, κ = 1.81. The experimental plasma current decay time was evaluated by using the following equation:

$$\tau_{100-80} = I_{p0}/(\Delta I_p/\Delta t). \qquad (1)$$

Here, I_{p0} is the plasma current just after the TQ, ΔI_p is 20% of I_{p0}, and Δt is the time interval between I_{p0} and $0.8I_{p0}$, respectively.

Evaluations of plasma resistance R_p and L_p are necessary to verify the current quench model during the initial phase of CQ in DIII-D tokamak. To evaluate the L_p during the initial phase of the CQ, we used the CCS code. CCS code can evaluate magnetic flux only outside plasma, and the shape of Last Closed Flux Surface (LCFS) and Shafranov lambda can be evaluated from evaluated magnetic flux [4]. For evaluation of L_p, following equations were used;

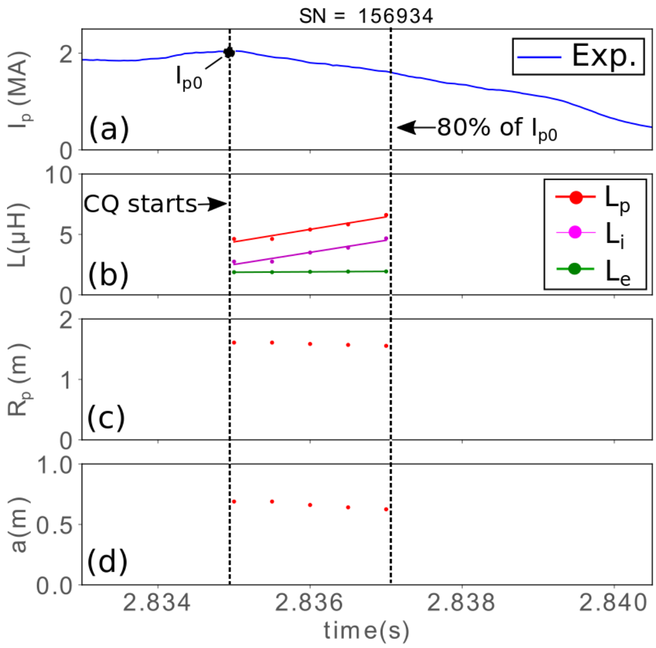

Fig. 1: Time evolutions of (a) the plasma current I_p, (b) the plasma inductance L, (c) the major radius R_0, and (d) minor radius a evaluated by CCS code during CQ.

$$L_p = L_i + L_e = \mu_0 R_0(\Lambda - \beta_p) + \mu_0 R_0(\ln(8R_0/a) - 2). \qquad (2)$$

Here, Λ is Shafranov lambda and β_p is the poloidal beta. In this study, we assumed $\beta_p = 0$ after the TQ. Fig.1 shows the time evolutions of plasma parameters evaluated by CCS code. In this discharge, the experimentally current decay time $\tau_{100\text{-}80}$ is 9.4 ms. As shown in Fig. 1 (b), it was found that L_p, especially L_i, was increased during the initial phase of CQ. Fig. 2 shows the relationship between the time derivative of L_i and CQ time during the initial phase of the CQ in 3 types of DIII-D disruptions. It was found that dL_i/dt was increased with decrease of CQ time similar to JT-60U results.

3. Comparison of CQ behaviour with the disruption simulation code

To investigate the mechanism of causing the increase of L_i, simulation of the CQ waveform by using the disruption simulation code DINA is necessary. The DINA code [5] is a two-dimensional free-boundary equilibrium evolution program with consideration of the external circuits (PF coils and surrounding conducting structures). A

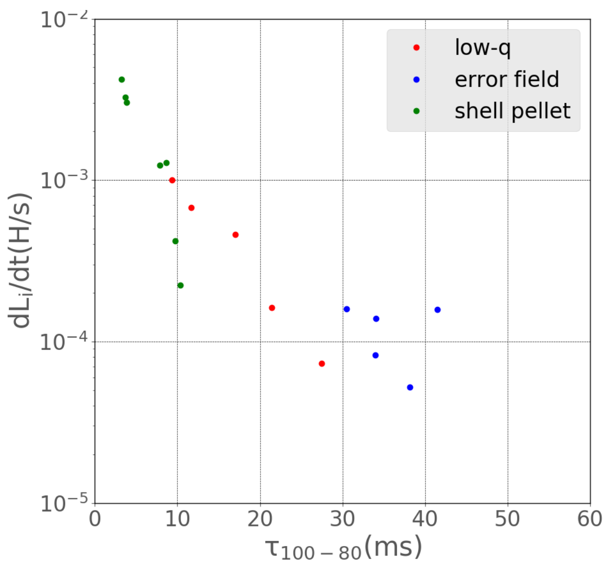

Fig. 2: The relationship between time derivative of L_i and CQ time during the initial phase of the CQ.

DIII-D version of the DINA code was set up for analysis of CQ. In this study, we started the DINA calculation from the time when the current quench starts. In DINA simulations, we set the initial parameters such as the shape of the LCFS and the current in the PF coils to match experimental data.

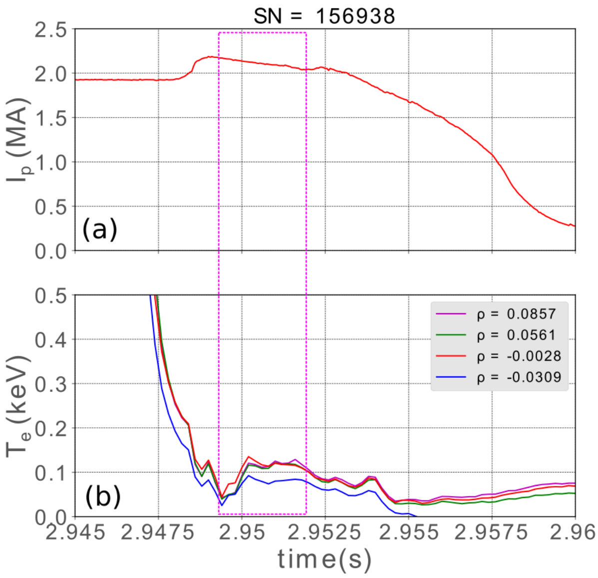

Fig. 3: Time evolution of electron temperatures in core region evaluated by ECE measurement in slow plasma current decay.

Fig. 3 shows the time evolution of T_e during the initial phase of CQ evaluated by ECE measurement. The experimental current decay time is 27.5 ms in this discharge and this is slow decay in this study. It was found that T_e over 100eV at the plasma center have been observed in slow decay. T_e except the core region could not be measured using ECE because the optical thickness is small at T_e < 100 eV in DIII-D. Thus, we assumed various T_e profile with the core T_e = 100 eV in DINA simulations. Fig. 4 (a) shows the various T_e profiles assumed during the CQ in DINA simulations. T_e profiles were assumed by using the following equation;

$$T_e(\rho) = 100(1-\rho^2)^\nu + 10. \qquad (3)$$

In these simulations, we assumed that T_e profile doesn't change in time. Fig. 4 (b) shows the initial j profile in DINA simulations. α means an adjustable value related to peak index of j profile. The initial j profile changed into flat profile with a decrease of α. CQ analysis were carried out by using these initial j and assumed T_e profiles to investigate a mechanism of an increase of L_i during the initial phase of CQ.

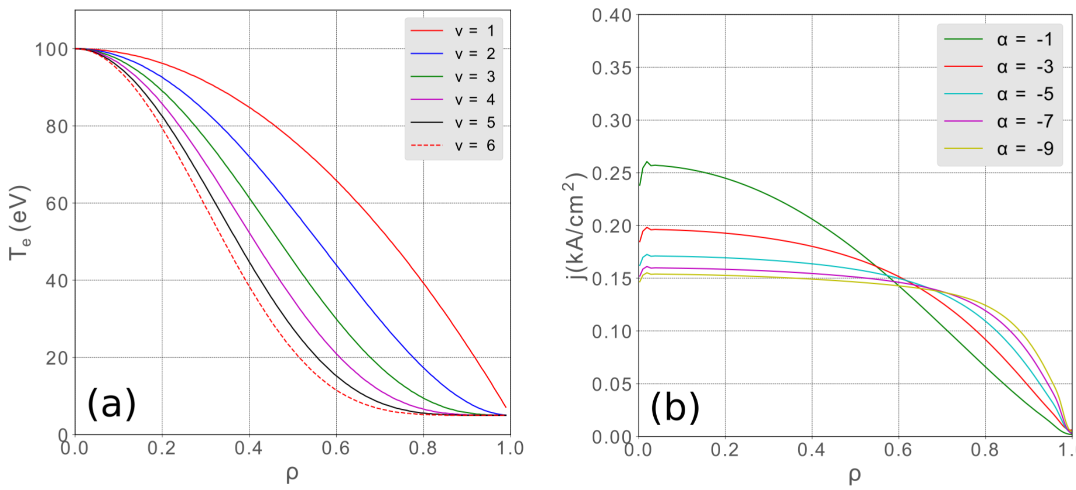

Fig. 4: (a) Assumed T_e profile during the initial phase of CQ and (b) the initial current density profiles j in DINA simulation.

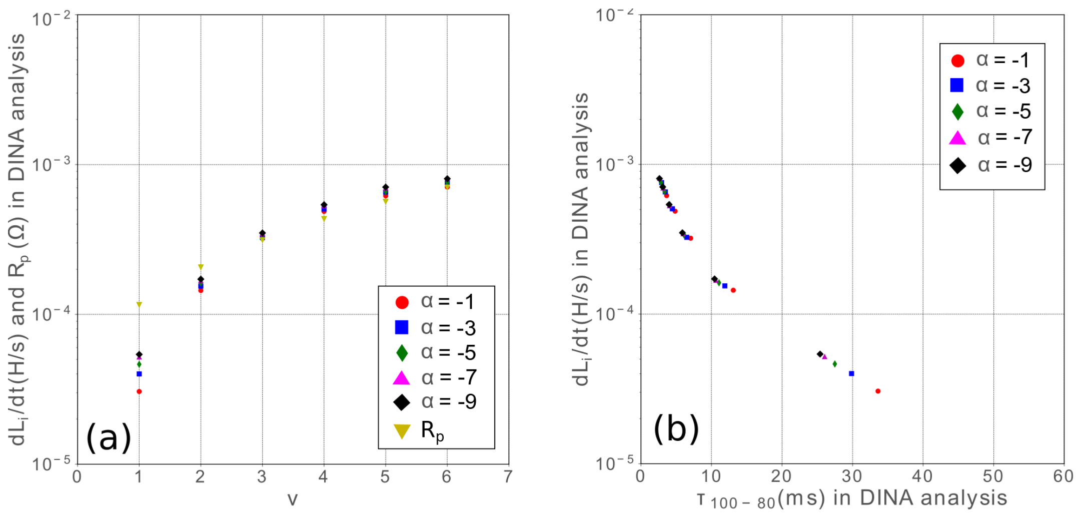

Fig. 5: (a) Relationship between ν in assumed T_e profile and dL_i/dt, R_p in DINA analysis. (b) Relationship between current decay time and dL_i/dt in DINA analysis.

Fig. 5 (a) shows the relationship between peak index ν of assumed T_e profile and dL_i/dt in DINA analysis. It was found that differences in the T_e profile shape affects the increase of L_i during CQ and difference of initial j profile has a weak influence for the increase of L_i. The area-averaged R_p in this figure was calculated from assumed T_e profile by using Spitzer resistivity [6]. Calculation results of dL_i/dt except $\nu = 1$ were almost the same value with values of R_p. Fig. 5 (b) shows the relationship between current decay time and dL_i/dt in DINA analysis similar to Fig. 2. In these results, the increase of L_i and the plasma current decay were in agreement with the experimental data in slow decay when peak index ν of assumed T_e profile was 1. It was found from these DINA calculations that the T_e profile was important to generate the increase of L_i during CQ and dL_i/dt affect the current decay during CQ in DIII-D because dL_i/dt and R_p were almost same values.

4. Summary

In this study, we analyzed current quenches in 3 types of DIII-D disruptions to investigate the determination mechanism responsible for the initial phase of current quench in DIII-D tokamak. It was found that dL_i/dt during the initial phase of CQ was increased with a decrease of CQ time, identical to JT-60U results. The T_e profile was important to generate the increase of L_i and dL_i/dt affects the current decay during CQ in DIII-D. This material is based upon work supported by the US Department of Energy under Award Number(s) DE-FC02-04ER54698 and Japan / U. S. Cooperation in Fusion Research and Development.

[1] T. C. Hender, *et. al.*, Nucl. Fusion **47** S128-202 (2007). [2] Y. Shibata, *et. al.*, Nucl. Fusion **50**, 025015 (2010).
[3] Y. Shibata, *et. al.*, Plasma Phys. Cont. Fusion **56** 045008 (2014).
[4] K. Kurihara, Fusion Eng. Des., **51-52**, 1049 (2000).
[5] R. Khayrutdinov and V. Lukash, J. Comput. Phys. **109** 193(1993).
[6] Spitzer L and H¨arm R Phys. Rev. **89** (1953) 977.